13.1;07.3

Stability of functional characteristics of transparent electrodes based on the ZnO : Ga/Ag/ZnO : Ga multilayer structure

© A.Sh. Asvarov[1,2], A.K. Akhmedov[1], A.E. Muslimov[2], V.M. Kanevsky[2]

1 Amirkhanov Institute of Physics, Dagestan Federal Research Center, Russian Academy of Sciences, Makhachkala, Russia
[2] Shubnikov Institute of Crystallography „Crystallography and Photonics" Russian Academy of Sciences, Moscow, Russia
E-mail: abil-as@list.ru

Received August 23, 2021
Revised September 29, 2021
Accepted October 20, 2021

Since the stability of functional properties of a transparent conducting three−layer structure ZnO:Ga/Ag/ZnO:Ga is important for practical application, we studied its long-term durability and thermal stability in air environment. It has been demonstrated that after prolonged interaction with the air environment at room temperature (for ~ 1000 days) and further heat treatment in air at temperatures of up to 450°C (for up to 10 h), the three−layer structure retains its integrity and is characterized by a low sheet resistance $R_s = 2.8\,\Omega$/sq at average transmittance in the visible range $T_{av} = 82.1\%$.

Keywords: transparent electrode, multilayer structure, ZnO, Ag, Ga, sheet resistance, transparence, stability, heat treatment.

DOI: 10.21883/TPL.2022.01.52481.19001

Transparent electrodes are important components of many optoelectronic devices [1]. Recently, along with conventional materials for transparent electrodes based on wide−bandgap oxides (In_2O_3, SnO_2, ZnO, TiO_2), great interest is attracted also by three−layer structures in which between two oxide layers there is an ultrathin continuous layer of Cu, Ag, Au, etc. [2,3]. The metal layer continuity in such structures provides record−breaking low values of the total specific resistance ($10^{-5}\,\Omega \cdot$ cm) that are an order of magnitude lower than those characteristic of conventional oxide−based transparent electrodes. What is also important is that formation of such structures does not typically need heating of the substrates, which provides great opportunities for their commercial fabrication on polymer substrates. In addition, the technique of DC magnetron sputtering widely used in opto— and microelectronics suits well their layer−by−layer formation.

However, in estimating the possibility of using one or another material as a transparent electrode it is important to know how their functional characteristics change during their direct contact with the environment and in the process of various thermal treatments. Though stability of conventional transparent conducting electrodes based on wide−bandgap oxides is already well studied [4,5], the question about time stability of characteristics of multilayer transparent conducting structures needs further investigation [6].

Earlier, in 2019, we performed optimization of thicknesses of the oxide layers and silver interlayer of the three−layer symmetric system ZnO : Ga/Ag/ZnO : Ga (GAG) so as to reach the maximal FOM (figure of merit) $= T_{av}^{10}/R_s$ (where T_{av} is the mean optical transmittance, R_s is the sheet resistance of the transparent electrode) [7]. We have shown that, when the optimized oxide layer thickness is $d_{GZO} = 40$ nm and thickness of the ultrathin intermediate silver layer is $d_{Ag} = 10$ nm (Fig. 1, *a*), the three−layer GAG structure whose fabrication details are presented in [8] is characterized by low sheet resistance $R_{s0} = 2.45\,\Omega$/sq, high transparence $T_{av0} = 81.3\%$ and record−breaking FOM criterion $\mathrm{FOM}_0 = 5.2 \cdot 10^{-2}\,\Omega^{-1}$. Therewith, the bottom oxide layer $d_{GZO} = 40$ nm thick provided early coalescence of Ag nucleation centers and formation of a continuous metal nanofilm, Fig. 1, *b*) characterized by minimal light scattering from discontinuities (pores, large aggregates, etc.); jointly with the identical top oxide layer, the interlayer ensured the maximal antireflection effect [9].

This paper presents the results of studying stability of functional characteristics of the given GAG structure during aging (indoor storage for 33 months at the mean temperature of 24°C and mean relative humidity of 65%) and also during annealing in air at the temperatures of up to 450°C (in the tube−type furnace Nabertherm RD 30/200/11, Germany).

In general, visual examination of the samples after aging and thermal treatment has not revealed any signs of degradation, except for the edge regions (up to 1 mm from the substrate edge) where the structure delamination was observed after annealing at 450°C; the delamination was connected with silver oxidation due to lateral diffusion of oxygen through the three−layer structure butt end.

After the long−term storage of the sample, no variations in its microstructure were revealed. The diffractogram of the aged sample, as well as that of the initial sample, exhibited two main reflexes located at 34.10 and 38.25° which were related to reflection from plane (002) of the ZnO hexagonal lattice and plane (111) of the Ag cubic lattice, respectively.

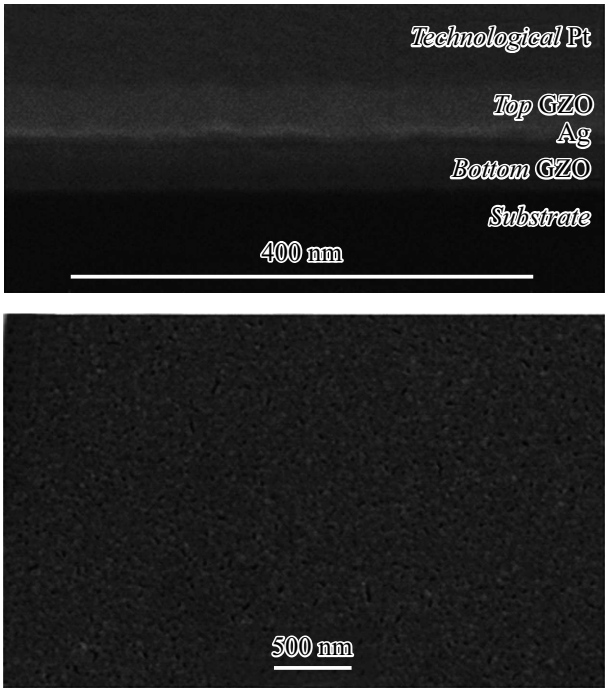

Figure 1. SEM microphotos of the transverse cleave of the three–layer GAG structure with the optimized layer thicknesses (a) and of the surface of a 10 nm thin Ag film deposited on the ZnO : Ga (GZO) film 40 nm thick (b).

The aged sample diffractogram did not exhibit new reflexes, while the location and shape of two already revealed reflexes remained the same (Fig. 2, a).

In their turn, subsequent annealings of the aged sample led to structural variations. The increase in the annealing temperature and duration caused a considerable shift of the 002 ZnO reflex position towards the tabular value ($2\theta_0 = 34.40°$) and also a slight amplitude increase and width decrease, which evidences an improvement in the ZnO phase crystallinity. As for the 111 Ag reflex, annealing did not change its location but caused essential variations in its shape. After annealing at 350°C, the reflex is characterized by the presence of smooth right and left shoulders and scarcely pronounced peaks on the reflex maximum (indicated by arrows in Fig. 2, a), which means that a few less intense reflexes are superimposed on the main 111 Ag reflex (see the Fig. 2 inset). This complex shape of the reflex may be explained either by partial silver oxidation with formation of the Ag_2O_3 [10] and Ag_2O [11] phases or by formation in the metal interlayer of several populations of Ag nanocrystallites with different sizes of coherent scattering regions [12,13]. The observed decrease in the width of main reflex 111 Ag (at 0.64° for the initial and aged samples and at 0.56° for the annealed samples) may be explained by reduction of microdeformations of the Ag nanocrystalline lattices and an increase in their mean size. A slight decrease in the 111 Ag reflex intensity relative to that of the 002 ZnO reflex after the final annealing at 450°C may be an evidence of partial escape of silver into the neighboring oxide layers and increase in the fraction of partly oxidized silver.

Comparison of the optical spectrometry data for the initial and aged samples showed that the bell shape of the initial sample spectrum changed scarcely after storing for 33 months (Fig. 2, b). While maximum transmittance $T_{max} = 89.5\%$ for the initial sample was observed at the wavelength $\lambda_{max} = 528$ nm, the sample aging resulted in slight reduction of the height of the bell–shaped transmission band and in a rightward shift of its maximum ($T_{max} = 87.5\%$, $\lambda_{max} = 542$ nm).

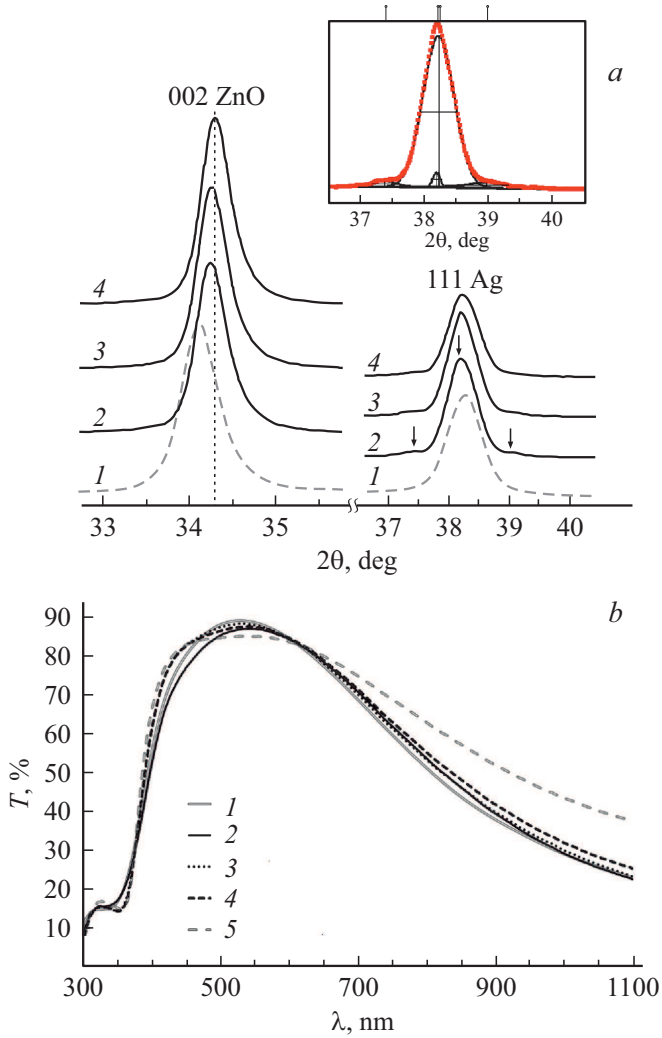

Figure 2. a — sections of the GAG sample diffractograms with reflexes 002 ZnO and 111 Ag. *1* — the aged sample, *2* — the sample after two–hour annealing at 350°C, *3* — the sample after ten–hour annealing at 350°C, *4* — the sample after two–hour annealing at 450°C. The inset presents a case of decomposition of a complex–shape reflex located at $2\theta = 38.25°$. b — optical transmission spectra of the GAG three–layer structure immediately after sputter deposition (*1*), after long–term storage (*2*), after the first two–hour annealing in air at 350°C (*3*), after the subsequent ten–hour annealing at 350°C (*4*) and after the final two–hour annealing in air at 450°C (*5*).

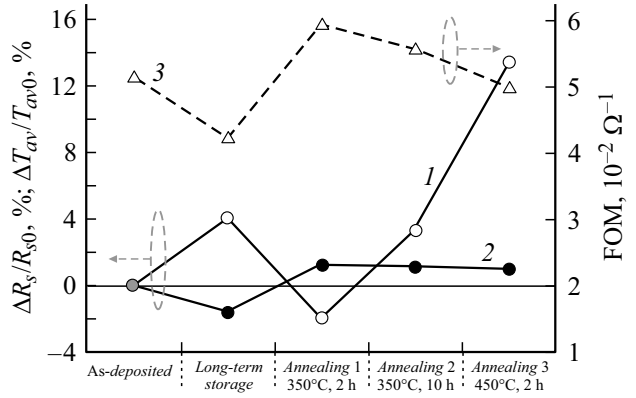

Figure 3. Relative variations in the sheet resistance $\Delta R_s/R_{s0}$ (*1*), mean optical transmittance for the 400−700 nm range $\Delta T_{av}/T_{av0}$ (*2*) and variation in the figure of merit FOM (*3*) due to long−term storage and annealing.

The following two−hour annealing in air at 350°C results in broadening of the bell−like transmission band mainly due to an increase in the violet spectrum range. $T_{\max}$ reaches 88.9% at $\lambda_{\max} = 530$ nm.

The following annealings, namely, the ten−hour one at 350°C and next two−hour one at 450°C, caused an increase in the transmittance in the violet and orange−red spectrum ranges and slight reduction in the center of the visible range ($\lambda = 500-600$ nm) with retaining the transmission maximum location in the vicinity of $\lambda_{\max} = 540$ nm.

Fig. 3 demonstrates relative variations in the main functional characteristics of the GAG structure (mean transmittance T_{av} for the wavelength range of 400−700 nm and sheet resistance R_s), as well as absolute variation in the studied structure FOM after storage for 33 months and after exposure to subsequent anneals.

One can see that after long−term storage sheet resistance R_s increased by $\sim 4\%$ to the value of 2.55 Ω/sq, while transmittance T_{av} decreased by $\sim 2\%$ as compared with corresponding values for the initial sample. This results in the FOM decrease due to the sample aging by 18% and getting the value of $4.2 \cdot 10^{-2}\,\Omega^{-1}$. Since the aged GAG sample does not exhibit structural variations and demonstrates only scarce variations in the post−aging transmission spectrum, it is possible to assume that reduction of the three−layer structure functional characteristics is caused by variations in electrical and optical properties of the thin top oxide layer. Degradation of electrooptical properties of the ZnO−based layer may be connected with surface states of the ZnO nanocrystallites. It is known that the ZnO−based transparent conducting layers up to 100 nm thick do not exhibit high stability of electrical characteristics in contacting the environment [14]. Absorption of oxygen and water molecules at the grain−grain interfaces causes degradation of electrical properties of thin ZnO films due to enhancement of charge carriers scattering from the grain−grain interfaces. Along with this it is known that properties of the ZnO : Ga transparent conducting films are nevertheless more stable than those of undoped ZnO and ZnO : Al [5,15].

The following two−hour aged sample annealing in air at 350°C FOM provides a considerable FOM increase to $5.9 \cdot 10^{-2}\,\Omega^{-1}$ which is higher than FOM_0. The observed FOM increase caused by simultaneous reduction of R_s and growth of T_{av} may be explained by annealing of multiple ZnO and Ag defects characteristic of the layers deposited at relatively low temperatures [6]. Annealing of defects leads to reduction of light scattering and also of scattering of charge carriers inside the crystallites and on their boundaries. During annealing, the top oxide layer efficiently prevents the oxidant delivery to the ultrathin Ag layer that is the main supplier of free charge carriers in the three−layer structure.

As a result of two further intense thermal treatments, despite T_{av} remains high, $\Delta R_s/R_{s0}$ increases monotonically by $\sim 14\%$ ($R_s = 2.8\,\Omega$/sq), which leads to a slight FOM decrease to $5.0 \cdot 10^{-2}\,\Omega^{-1}$. The sheet resistance increase may be caused by partial oxidation of silver and by mutual diffusion between the layers. It is known that when ZnO is doped with silver, its conductivity can decrease by a few orders of magnitude [16].

Notice that our investigation did not reveal fatal destruction of the three−layer structure caused by transformation of the continuous silver layer into separate large grains or by its total oxidation in the process of annealing at temperatures above 300°C [6,17]. Those papers noticed that adding low amounts of Al to silver in the ZnO/Ag/ZnO multilayer structures inhibits silver aggregation and interdiffusion between the metal and oxide layers, which increases considerably the thermal stability. In the case of the GAG three−layer structure it is possible to assume that the role of such an inhibitor may be played by Ga diffusing during annealing from the oxide layers to the inter-layer interfaces and directly into the silver layer. High stability of three−layer structures in which thin ZnO : Ga films are used as oxide components was emphasized also by other researchers [18].

Thus, in this work we have studied stability of functional characteristics of transparent conducting structure ZnO : Ga/Ag/ZnO : Ga fabricated by magnetron sputtering on an unheated substrate during its long−term contact with the environment and in the process of subsequent thermal treatments in open air. High stability of the three−layer structure with optimized thicknesses of its layers has been demonstrated. In 33 months after deposition, the sheet resistance increased by 4%, while the visible−range transparence decreased by 2%. Also it has been shown that atmospheric annealing of the multilayer structure at the temperatures of up to 350°C promotes improvement of its functional characteristics. High stability of the ZnO : Ga/Ag/ZnO : G three−layer structures opens wide opportunities for implementing various−purpose transparent electrodes based on these structures.

Financial support

The studies were accomplished in the scope of State Assignments of DFRC RAS and „Crystallography and Photonics“ FRC and was partly supported by Russian Fundamental Research Foundation (№ 20-02-00373, 20-21-00068) as well as by the RF Ministry of Education and Higher Education (Agreement № 075-15-2021-1362) with involving equipment of Analytical Common Use Center RAS and Common Use Center „Structural Material Diagnostics “ of FRC „Crystallography and Photonics“ RAS.

Conflict of interests

The authors declare that they have no conflict of interests.

References

[1] A.I. Baranov, D.A. Kudryashov, A.V. Uvarov, I.A. Morozov, A.A. Maksimova, E.A. Vyacheslavova, A.S. Gudovskikh, Pis'ma v ShTF, **47** (16), 24 (2021) (in Russian). DOI: 10.21883/PJTF.2021.16.51324.18779
[2] G. Lucarelli, T.M. Brown, Front. Mater., **6**, 310 (2019). DOI: 10.3389/fmats.2019.00310
[3] Z. Zhao, T.L. Alford, Solar Energy Mater. Solar Cells, **157**, 599 (2016). DOI: 10.1016/j.solmat.2016.07.044
[4] H. Beh, D. Hiller, J. Laube, S. Gutsch, M. Zacharias, J. Vac. Sci. Technol. A, **35**, 01B127 (2017). DOI: 10.1116/1.4972466
[5] H. Akazawa, J. Vac. Sci. Technol. A, **35**, 041515 (2017). DOI: 10.1116/1.4990538
[6] L. Liu, S. Ma, H. Wu, B. Zhu, H. Yang, J. Tang, X. Zhao, Mater. Lett., **149**, 43 (2015). DOI: 10.1016/j.matlet.2015.02.093
[7] A. Anand, M.M. Islam, R. Meitzner, U.S. Schubert, H. Hoppe, Adv. Energy Mater., **11**, 2100875 (2021). DOI: 10.1002/aenm.202100875
[8] A.K. Akhmedov, A.K. Abduev, V.M. Kanevsky, A.E. Muslimov, A.S. Asvarov, Coatings, **10**, 269 (2020). DOI: 10.3390/coatings10030269
[9] F. Hajakbari, M. Ensandoust, Acta Phys. Pol. A, **129**, 680 (2016). DOI: 10.12693/ APhysPolA.129.680
[10] X.-Y. Gao, S.-Y. Wang, J. Li, Y.-X. Zheng, R.-J. Zhang, P. Zhou, Y.-M. Yang, L.-Y. Chen, Thin Solid Films, **455-456**, 438 (2004). DOI: 10.1016/j.tsf.2003.11.242
[11] P. Wang, D. Zhang, D.H. Kim, Z. Qiu, L. Gao, R. Murakami, X. Song, J. Appl. Phys., **106**, 103104 (2009). DOI: 10.1063/1.3259426
[12] C.F. Holder, R.E. Schaak, ACS Nano, **13**, 7359 (2019). DOI: 10.1021/acsnano.9b05157
[13] T. Miyata, Y. Ohtani, T. Kuboi, T. Minami, Thin Solid Films, **516**, 1354 (2008). DOI: 10.1016/j.tsf.2007.03.084
[14] A. Asvarov, A. Abduev, A. Akhmedov, A. Abdullaev, Phys. Status Solidi C, **7**, 1553 (2010). DOI: 10.1002/pssc.2009831581
[15] L. Xu, J. Miao, Y. Chen, J. Su, M. Yang, L. Zhang, L. Zhao, S. Ding, Optik, **170**, 484 (2018). DOI: 10.1016/j.ijleo.2018.06.016
[16] L. Zhou, X. Chen, F. Zhu, X.X. Sun, Z. Sun, J. Phys. D: Appl. Phys., **45**, 505103 (2012). DOI: 10.1088/0022-3727/45/50/505103
[17] C. Zhang, J. Zhao, H. Wu, S. Yu, J. Alloys Compd., **832**, 154983 (2020). DOI: 10.1016/j.jallcom.2020.154983
[18] S.H. Lee, G. Kim, J.W. Lim, K.-S. Lee, M.G. Kang, Solar Energy Mater. Solar Cells, **186**, 378 (2018). DOI: 10.1016/j.solmat.2018.07.010